Structural Chemistry
https://doi.org/10.1007/s11224-022-01935-x

ORIGINAL RESEARCH

Calcium coordination compounds of anionic forms of hydrogen dipicolinate and quinolinate: synthesis, characterization, crystal structures and DFT studies

Adedibu C. Tella[1,2] · Adetola C. Oladipo[1,3] · Victoria T. Olayemi[1,4] · Allen Gordon[5] · Adeniyi S. Ogunlaja[5] · Lukman O. Alimi[6] · Stephen P. Argent[7] · Robert Mokaya[7] · Guy J. Clarkson[8] · Richard I. Walton[8]

Received: 21 January 2022 / Accepted: 4 April 2022
© The Author(s), under exclusive licence to Springer Science+Business Media, LLC, part of Springer Nature 2022

Abstract

Two calcium coordination compounds $[Ca(2,6\text{-}Hpdc)_2(H_2O)_2]$ **1** and $[Ca_2(2,3\text{-}pdc)_2(H_2O)_6]_n$ **2** (where 2,6-H_2pdc = 2,6-pyridinedicarboxylic acid and 2,3-H_2pdc = 2,3-pyridinedicarboxylic acid) were grown at room temperature. The compounds were characterized using elemental analysis, Fourier transform infrared (FTIR) spectroscopy, thermogravimetric analysis, powder X-ray diffraction and single crystal X-ray crystallographic analysis. The structures of both compounds are stabilized by a network of hydrogen bonds arising from coordinated water molecules and carboxylate groups. Computational analysis revealed that compound **1** has a large energy gap (9.221 eV), suggesting high excitation energies and chemical hardness making it a better electron acceptor while compound **2** displayed a smaller energy gap (5.156 eV), which is indicative of a softer molecule with better polarizability and reactivity.

Keywords Alkaline earth metals · Molecular orbitals · Pyridine carboxylate · Calcium coordination compounds

Introduction

There has been wide development of coordination compounds, composed of metal centres and organic ligands which are able to extend in different dimensions. Their relevance in many fields like organic and inorganic chemistry, biochemistry, material science, electrochemistry and pharmacology with many potential applications, such as catalysis, magnetism, adsorption, luminescence and biology applications has led to extensive study of these compounds [1, 2]. Furthermore, the need for cheap ssand less toxic coordination compounds for biological applications has necessitated the use of alkaline earth metals [3, 4]. Specifically, calcium is useful in biological processes such as carbohydrate metabolism, enzyme activation and nucleic acid complexation as it is an essential constituent in living organisms [5]. Other applications of calcium-based compounds include sensing [6], catalysis [7] and adsorption of gases [8].

In the same way, ligands with mixed-functionalities such as pyridinecarboxylate, pyrazinecarboxylate and imidazolecarboxylate have been reported to favor the design of diverse structure of coordination compounds with fascinating potential applications [9–11]. Furthermore, these ligands are known to possess strong and weak hydrogen bonding

✉ Adedibu C. Tella
ac_tella@yahoo.co.uk

1 Department of Chemistry, University of Ilorin, Kwara State, P.M.B.1515, Ilorin, Nigeria

2 Department of Chemistry, University of South Africa, Pretoria, South Africa

3 Department of Physical Sciences, Industrial Chemistry Programme, Landmark University, Kwara State, P.M.B.1001, Omu-Aran, Nigeria

4 Department of Chemistry, Faculty of Pure and Applied Sciences, Kwara State University, P.M. B 1530, Malete, Nigeria

5 Department of Chemistry, Nelson Mandela University, P.O. Box 77000, Port Elizabeth 6031, South Africa

6 Department of Chemistry and Polymer Science, Stellenbosch University, Western Cape, Stellenbosch 7602, South Africa

7 School of Chemistry, University of Nottingham, University Park, Nottingham NG7 2RD, UK

8 Department of Chemistry, University of Warwick, Coventry CV4 7AL, UK

Published online: 12 April 2022

(such as O–H···O and C-H····O) and π- π stacking interactions, which influence their biological properties [12–15].

The syntheses of calcium compounds of trimellitate ligand have been reported in the literature [16–19]. Calcium coordination polymer was built up from infinite chains of calcium polyhedra interconnected to each other through the trimellitate ligands [16]. Four three-dimensional (3D) calcium-based coordination compounds were constructed from 2,5-dibromoterephthalic acid. The tuning and formation of different network topologies were explored by the introduction of different N-donor organic species as additional auxiliary ligands to the system, the fluorescence properties of the compounds were also reported [17]. In a report, calcium coordination compounds of three different chlorophenoxyacetic acids (3-chlorophenol, 4-chloro-2-methylphenol, 2,4,6-trichlorophenol) were synthesized. Differences in the number and position of the chlorine substituents were reported to lead to diversities in the crystal structures of the three calcium compounds obtained. Furthermore, a steric hindrance effect and the formation of O–H···Cl hydrogen bond contributed to the enrichment of the structures [18]. A Ca(II) coordination compound of L-malic acid was synthesized and reported to have high thermal stability. In addition, the compound is capable of emitting its own characteristic sensitized luminescence [19].

Despite these existing reports, there are still fewer reports on coordination compounds of alkaline earth metals compared to those of transition metals, this is because their geometries are not predictable as their bonding mode is not governed by ligand field stabilization [20].

Carboxylates of s-block metals have high affinity for oxygen donor, e.g. water [20]. Many researchers have reported their synthesis is aqueous media, e.g. hydrothermal synthesis [21–23]. Herein, we report the synthesis of two calcium coordination compounds, $[Ca(2,6\text{-}Hpdc)_2(H_2O)_2]$ **1** and $[Ca_2(2,3\text{-}pdc)_2(H_2O)_6]_n$ **2,** of dipicolinic and quinolinic acids (Fig. 1) in aqueous medium alongside suitable solvents, using solvothermal and room temperature synthetic reactions respectively. Furthermore, DFT study was employed to gain insight on the electronic properties of the compounds.

Experimental

Materials and methods

All reagents and chemicals were of analytical grade and were used as received without further purification. 2,3-pyridinedicarboxylic acid and 2,6-pyridinedicarboxylic acid were purchased from Sigma Aldrich, Germany. Calcium nitrate tetrahydrate ($Ca(NO_3)_2.4H_2O$) was supplied by Alfa Aesar, UK. Ethanol (98.8%), *N,N*-dimethyl formamide (DMF) (99.0%) were obtained from Central Drug House (P) Ltd, New Delhi, India.

Synthesis of the compounds

$Ca(2,6\text{-}Hpdc)_2(H_2O)_2$ 1

Compound **1** was prepared by dissolving 2,6-pyridinedicarboxylic acid (2,6-H_2pdc) (0.167 g, 1 mmol) and $Ca(NO_3)_2.4H_2O$ (0.118 g, 0.5 mmol) in two separate 50-mL beakers containing 10 mL ethanol and 10 mL distilled water, respectively. The solutions were mixed while stirring gently to obtain a clear colourless solution that was heated in an oven at 100 °C for 4 h under atmospheric conditions. The resulting clear colourless solution was kept standing undisturbed on the bench. White diamond-shaped crystals were obtained after 27 days. The crystals were separated from the mother liquor by filtration and washed in ethanol–water (2:1 by volume) solution and dried at room temperature for 30 min. Yield: 69%; $C_{14}H_{12}N_2O_{10}Ca$ (408.34 g/mol); Anal. found: C, 41.14, H, 2.76, N, 6.76%; Calc: C, 41.39, H, 2.48, N, 6.89%.; IR (cm^{-1}):3441, 3194, 1707, 1542, 1372, 540, 424.

$[Ca_2(2,3\text{-}pdc)_2(H_2O)_6]_n$ 2

Compound **2** was prepared by dissolving 2,3-pyridinedicarboxylic acid (2,3-pdc) (0.334 g, 2 mmol) and $Ca(NO_3)_2.4H_2O$ (0.236 g, 1 mmol) in two separate 50-mL beakers containing 10 mL distilled water and 10 mL DMF, respectively. The solutions were mixed together and stirred for 2 h at ambient temperature. The resulting clear colourless solution was kept standing

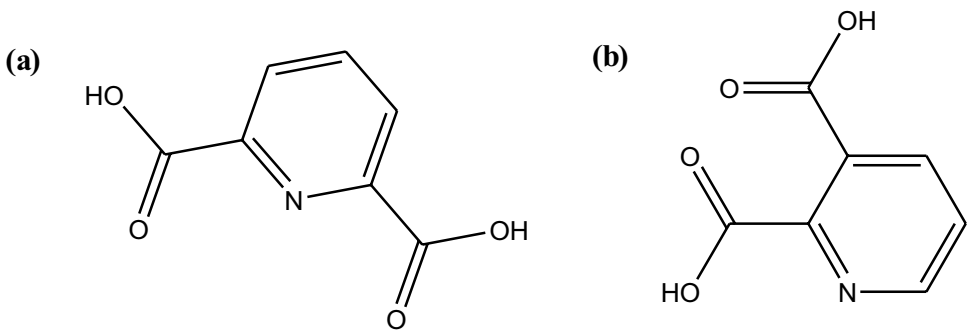


Fig. 1 Structures of **a** dipicolinic acid; **b** quinolinic acid

undisturbed on the bench. Colourless block-shaped crystals were formed after 22 days, filtered out of the solution and washed in ethanol–water (2:1 by volume) solution and dried at room temperature for 30 min. Yield: 76%; $C_{14}H_{18}N_2O_{14}Ca_2$ (518.46 g/mol); Anal. found: C, 32.87 (32.43); H, 3.39 (3.47); N, 5.46% (5.41); Calc: C,32.43; H, 3.47; N, 5.41%.; IR; (cm^{-1}): 3412, 2904, 1562, 1454, 1332, 662, 497.

Instrumentation and characterization

The samples were characterized by elemental analysis using an Exeter Analytical CE-440 Elemental Analyser. The infrared spectra were recorded using a Bruker Alpha diamond module FTIR spectrometer with attenuated total reflectance (ATR) attachment for solid samples. Powder X-ray diffraction (PXRD) patterns were measured on a PANalytical X'Pert PRO diffractometer with a Cu-Kα source (40 kV, 40 mA) with a step size of 0.02° and a 50 s time step. TGA was performed using an SDT-Q600 TA instrument. The samples were heated in air with a heating rate of 10 °C min^{-1} and the scan was recorded within the temperature range of 30–800 °C. Single crystal X-ray data for **1** were collected at 120 K on an Oxford Diffraction GV1000 diffractometer equipped with an Atlas S2 detector and mirror monochromated microfocus Cu source while **2** was collected at 150 K on Agilent Xcalibur Gemini diffractometer with a Ruby CCD area detector. Olex2 suite was used as a graphic user interface (GUI) and Mercury 4.0 as imaging software [24, 25]. The structures were solved with the ShelXT [26] structure solution program using intrinsic phasing and refined with the ShelXL [27] refinement package using least squares minimisation. All non-hydrogen atoms were refined with anisotropic displacement parameters.

Computational details

Theoretical studies were performed for **1** and **2**. The input files were taken from the CIF obtained from reported X-ray single crystal measurements. The geometries were optimized by minimizing energies with respect to all geometrical parameters without imposing any molecular symmetry constraints. Computational studies were carried out using the Gaussian 09 software package [28]. The calculations were performed by using B3LYP method (standard hybrid density functional method) with a basis set of 6–311 + + G** (2p, 2d) level [29].

Results and discussion

Structural description

The crystal data and structure refinement parameters of **1** and **2** are given in Table 1.

Compound **1** crystallized in the orthorhombic space group *Pccn*. The asymmetric unit comprises of one crystallographically independent Ca(II) ion, one 2,6-H_2pdc anion and a coordinated water molecule. The Ca(II) centre coordinates to two oxygen atoms (O8) from two 2,6-H_2pdc ligands, two oxygen atoms (O11) from two half deprotonated carboxylate groups, two oxygen atoms (O13) from two coordinated water molecules and two nitrogen atoms (N1) from two 2,6-H_2pdc ligands resulting in a distorted dodecahedral geometry (Fig. 2a). Selected bond lengths and angles are given in Table S1. The Ca-O_{carb} distances are in the range 2.4446 (15) Å – 2.6891 (17) Å and Ca-N is 2.561**2** Å which are similar to those observed in reported calcium coordination compounds [17]. The Ca-O_{water} bond length is 2.3177 (16) Å. The O–Ca–O bond angles for Ca1 range from 58.40 (5)° to 173.79(8)° (Table S1). The carboxylate group angles O8-C7-O9 and O11-C10-O12 are 126.26(19)° and 125.32° respectively, which is slightly wider than the O = C-O angle of pure dipicolinic acid (123.81(9)°) [30], possibly due to distortion by metal ion coordination. Furthermore, the torsional angle between the carboxylate group and the pyridyl ring (C3–C2–C7–O8) is 173.0(3)° and it is indicative of antiperiplanar conformation [31].

Interestingly, the O11-H11 group of the half deprotonated carboxylic group forms a strong intermolecular hydrogen bond with adjacent carboxylate group (O11−H11•••O8 = 2.573**2** Å). The coordinated water also forms a network of intermolecular hydrogen bonds and acts as the hydrogen bond donor (O13−H13A•••O9) and (O13−H13B•••O9) with D···A distances of 2.834 Å and 2.724 Å respectively (Fig. 2b). The selected hydrogen bonding parameters for **1** are shown in Table S2. The crystal packing shows that the molecules are connected by hydrogen bonds from coordinated water molecules which help in stabilizing the structure (Fig. 2b). The entire framework is further stabilized by π···π stacking between the centroid of one pyridyl ring (*i*1) and the centroid of the adjacent pyridyl ring (*i*2) within a layer (Fig. S3 and Table S3).

Compound **2** belongs to the monoclinic system with space group *Pc*, with a dimeric formula $[Ca_2(2,3\text{-pdc})_2(H_2O)_6]_n$. It has two coordination centres [Ca1 and Ca2], inducing a complete deprotonation of H_2pdc, which in turn affects the structural functionalities of the carboxylic residues. The asymmetric unit comprises

Table 1 Crystal data, data collection and structure refinement details for **1** and **2**

Details	**1**	**2**
Empirical formula	$C_{14}H_{12}CaN_2O_{10}$	$C_{14}H_{18}Ca_2N_2O_{14}$
Formula weight	408.34	518.46
T (K)	120.01 (10)	150 (2)
Wavelength (Å)	1.54184	1.54184
Crystal system	Orthorhombic	Monoclinic
Space group	*Pccn*	*Pc*
Crystal size (mm^3)	0.443 × 0.202 × 0.163	0.22 × 0.16 × 0.12
a (Å)	9.8403 (9)	13.50490 (10)
b (Å)	12.1668 (12)	10.27230 (10)
c (Å)	12.7110 (10)	7.25040 (10)
α (°)	90	90
β (°)	90	104.4030 (10)
γ (°)	90	90
V ($Å^3$)	1521.8 (2)	974.209 (18)
Z	4	2
ρ_{calc} (g/cm^3)	1.782	1.767
μ/mm^{-1}	4.193	5.845
F(0 0 0)	840.0	536.0
2Θ range for data collection (°)	11.566 to 150.262	6.758 to 146.658
Radiation type	Cu Kα	Cu Kα
Index ranges	$-11 \le h \le 12, -15 \le k \le 14, -10 \le l \le 15$	$-16 \le h \le 16, -12 \le k \le 12, -8 \le l \le 8$
Data/restraints/parameters	1518/4/132	3625/9/300
Independent reflections	1518 [$R_{int} = 0.0308$, $R_{sigma} = 0.0275$]	3625 [$R_{int} = 0.0236$, $R_{sigma} = 0.0185$]
Goodness-of-fit on F^2	1.112	1.082
Reflections collected	3453	18,534
$R_1[I > 2\sigma(I)]$	0.0566	0.0172
${}_wR_2$ (all data)	0.1575	0.0465
Largest peak (e A^3)	0.92	0.17
Deepest hole (e A^3)	−0.77	−0.18

of two Ca(II) ions, two 2,3-H_2pdc anions and six coordinated water molecules (Fig. 3). The coordination number of Ca1 in **2** is seven, the polyhedron being pentagonal bipyramid formed by one N, O set from one 2,3-H_2pdc molecule, two oxygen atoms from two 2,3-pdc molecules and three oxygen atoms of three water molecules, one of which bridges Ca1 and Ca2. The coordination number of Ca2 is also seven (one N, O set from one 2,3-H_2pdc molecule, one oxygen atom from one 2,3-H_2pdc molecule, and four oxygen atoms of four water molecules (including the bridging water molecule) and exhibits pentagonal bipyramid geometry (Fig. 4).The angle Ca1-O1-Ca2 is 130.05°, which results in the Ca1-Ca2 distance of 4.5741 Å. The O–Ca–O bond angles for Ca1 and Ca2 range from 68.99(5)° to 149.00(5)° while the O-Ca-N bond angles are 130.25(6)° similar to what was obtained for some calcium compounds of nitrogen-containing ligands [32]. Distances were found to be 2.6142 Å (Ca–N), 2.3725- 2.4044 Å [Ca-Ocarb] and 2.3706–2.5049 Å [Ca-O (H_2O)]. The [Ca-Ocarb] distances are similar to those observed in calcium carboxylate coordination compounds [17]. Selected bond lengths and angles have been listed in Table S1.

There are two modes of coordination of the 2,3-H_2pdc residue. In the first mode around Ca1, one of the carboxylate groups (O101) coordinates monodentately and bridges Ca1 atom, while the other carboxylate group coordinates bidentately, with one of the oxygen atoms (O110) bridging a Ca1 atom and the other (O109) chelating another Ca1 atom with the pyridine nitrogen (N107). In the second mode around Ca2, both carboxylate groups coordinate monodentately, with the coordinating oxygen of one group (O201) bridging a Ca2 atom and the coordinating oxygen of the other group (O210) chelating another Ca2 atom with the pyridine nitrogen (N207). These features were observed in heteronuclear compounds of H_2pdc [9].

The distance between Ca atom and the chelating oxygen atom (O109) is slightly longer than that of the bridging oxygen atom (O110), indicating the stronger bond

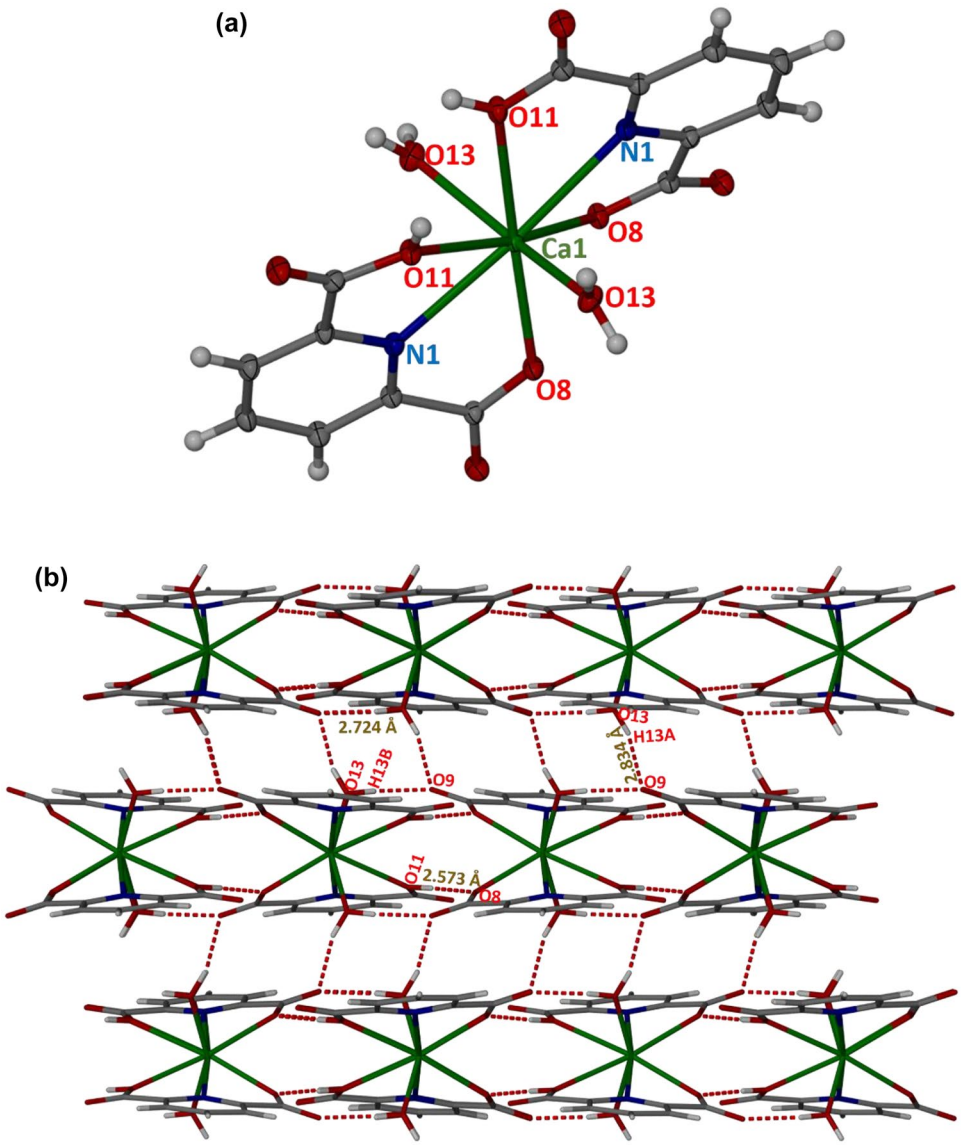


Fig. 2 **a** Displacement ellipsoid plot of **1** at 50% probability level; **b** packing arrangement showing O−H···O hydrogen bonding intermolecular interactions in **1** (red) along *a*-axis

of the latter. The plane of the carboxylic group of 2,3-H_2pdc ligand (C204–C203–C202–O201) is antiperiplanar with that of the aromatic ring, with a torsional angle of 103.08°. Apart from these interatomic distances between the centre metal and other heteroatoms, the crystal packing of compound **2** reveals there are O−H···O hydrogen bonding interactions between the coordinated water molecules and the carboxylate of the 2,3-H_2pdc molecules with donor–acceptor (D···A) distance in the range of 1.990–2.911 Å (Fig. 5 and Table S4). In addition to the O−H···O interactions, there exists C−H···O intermolecular interactions when viewed along the crystallographic *c*-axis. These interactions connect two adjacent 2,3-H_2pdc molecules involving the hydrogen atom from one 2,3-H_2pdc ring and oxygen atom of the carboxylate of the neighbouring 2,3-H_2pdc molecule (Fig. 6). The D···A distance is 3.458 Å.

Compound **2** possesses a 3D framework due to an extended system of hydrogen bonds involving carboxylates and coordinated water molecules as well as the perpendicular π···π interactions between the 2,3-pdc layers (Fig. S4 and Table S5). The 3D framework is shown in Fig. S5.

The powder X-ray diffraction (PXRD) data of compounds **1** and **2** were collected to ascertain their phase purity. The PXRD patterns of the as-synthesized samples were plotted against the simulated patterns as shown in Figs. S1 and S2. There was excellent agreement between the simulated and the experimental patterns which indicates high bulk purity of the as-synthesized phases.

FTIR studies

The comparison of the FTIR spectra of the free ligands and compounds **1** and **2** are shown in Figs. 7 and 8. For **1**, the

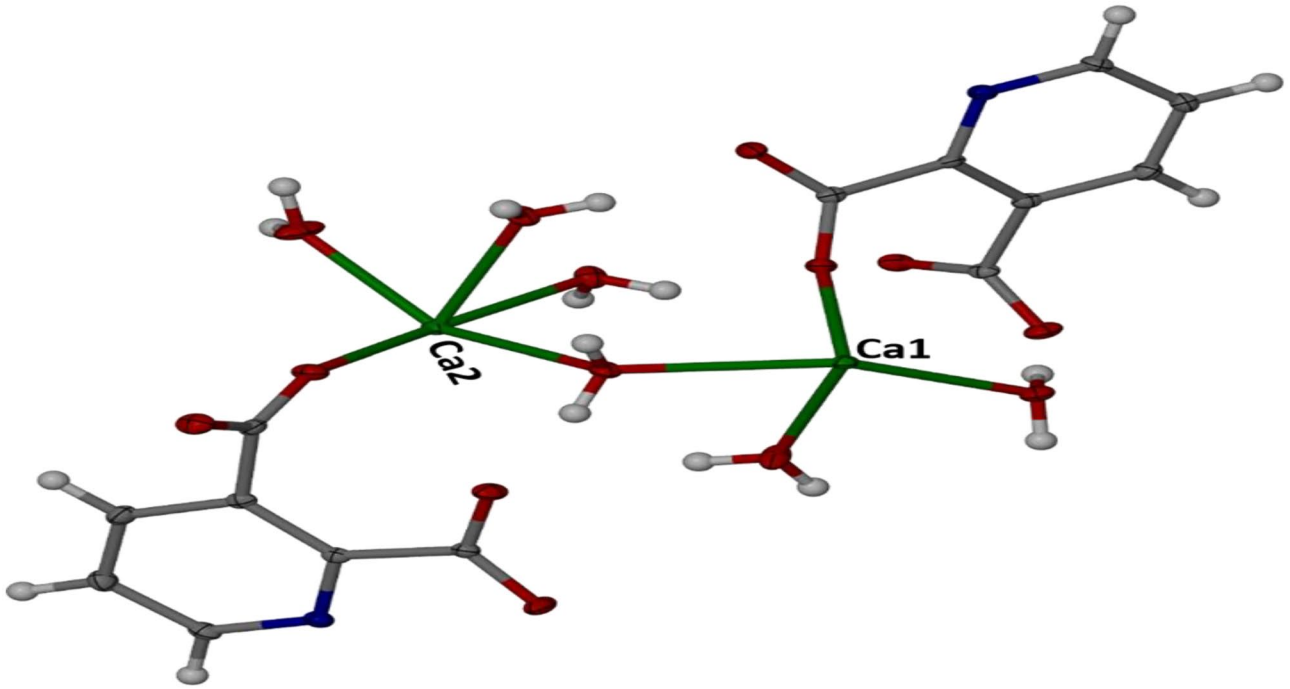


Fig. 3 Asymmetric unit of compound **2**

characteristic ν(C = O) and ν(C-O) absorption bands of the parent ligand were observed at 1583 and 1305 cm^{-1}. The absorption bands are shifted to higher and lower frequencies in the spectrum of **1**, 1707 cm^{-1} and 1291 cm^{-1} for ν(C = O) and ν(C-O) respectively indicating chelation of Ca(II) ion to the ligand. The asymmetric and symmetric vibrational bands

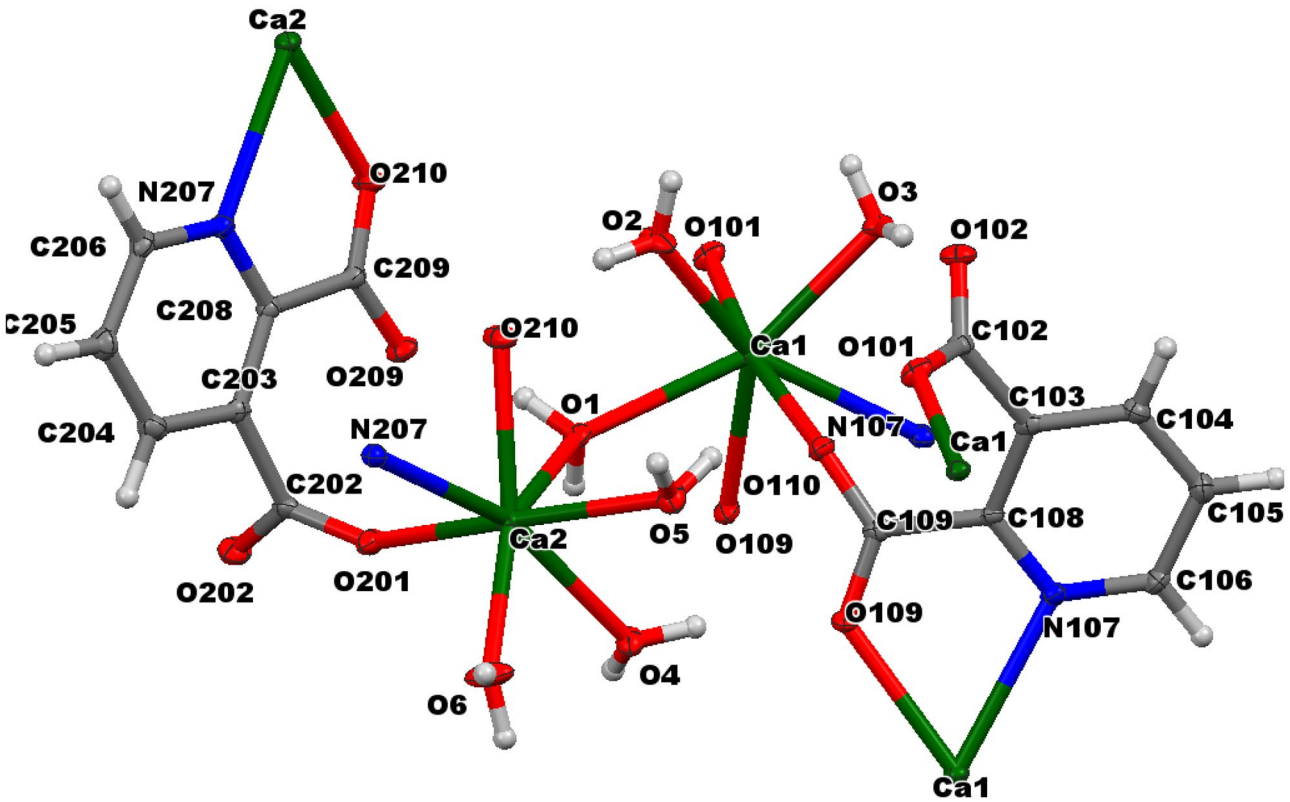


Fig. 4 Displacement ellipsoid plot of **2** drawn at 50% probability level

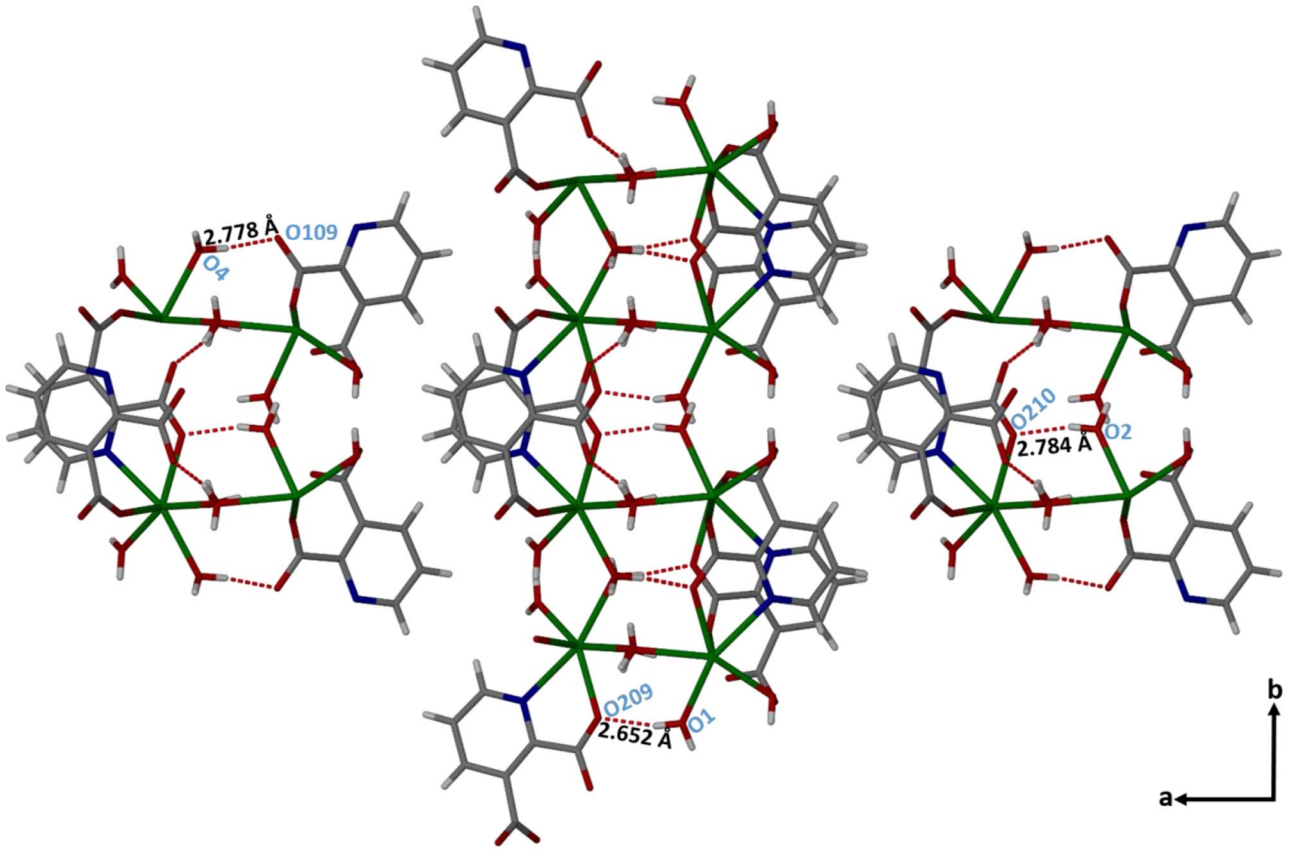


Fig. 5 Crystal packing of **2** showing O−H···O hydrogen bonding interactions when viewed along *c*-axis

are observed at 1543 and 1372 cm^{-1}. The calculated value $\Delta\nu(COO^-)$ is 171 cm^{-1}, confirming a multidentate coordination mode of the 2,6-H_2pdc ligand. However, the ν(C-N) found in the ligand at 1130 cm^{-1} is shifted to 1146 cm^{-1} in the spectrum of **1** due to coordination to the metal [33]. The broad band at 2571 cm^{-1} is assigned to O–H of carboxylic acid and is as a result of partial deprotonation of the ligand. The ν(O–H) for water is observed as a broad band at 3441 cm^{-1}.

The FTIR spectrum of **2** shows significant changes in absorption frequencies that occur at coordination sites, notably is the -OH band which appears around 3100 cm^{-1} in the spectrum of 2,3-H_2pdc but disappeared in that of compound **2** due to the coordination of the deprotonated -OH group to Ca (II) metal. The IR spectra shows useful information related to the carboxylate bands from the metal coordination compounds. 2,3-H_2pdc exhibits the typical $\nu(C=O)$ stretching mode in the 1700–1730 cm^{-1} range [34] absent in the spectrum of **2**, with new bands appearing at 1650 cm^{-1} and 1332 cm^{-1} for the $\nu_{asymmetric}(COO^-)$ and $\nu_{symmetric}$ (COO^-) respectively, validating the monodentate coordination of the carboxylate group. The vibrational frequency at 1580 cm^{-1} is ascribed to $\nu(C=N)$. This is shifted in the spectrum to 1562 cm^{-1} in compound **2**. The presence of coordinated water molecules is shown in the appearance of a new broad characteristic peak of O–H of water molecules around 3400 cm^{-1}. New bands observed at 497 cm^{-1} and 662 cm^{-1} are those of Ca-O and Ca-N respectively. The bands of ν(C–H) vibration modes also appear in this range 3087–2904 cm^{-1} and partially overlap with the bands of water molecules.

Thermal analysis

The TGA curves of compounds **1** and **2** are presented in Fig. 9. TGA curve of **1** shows a mass loss between 213 and 292 °C (56.10% found (calc. 50.49%)) assigned to the loss of two water molecules and a molecule of 2,6-H_2pdc ligand. The large difference between the experimental and calculated values may suggest the presence of excess surface water. A steady mass loss was further observed up to 474 °C (22.90% found (calc. 19.55%)) after which the framework collapsed leaving behind a residue of CaO. Compound **2** shows three thermal mass loss stages. The six molecules of water are lost in the first step, and this amounts to 21% (20.8%) of the total weight. The two 2,3- H_2pdc residues of weight 54% were lost in two indistinct steps, first between 400 and 530 °C and the second between 530 and 725 °C.

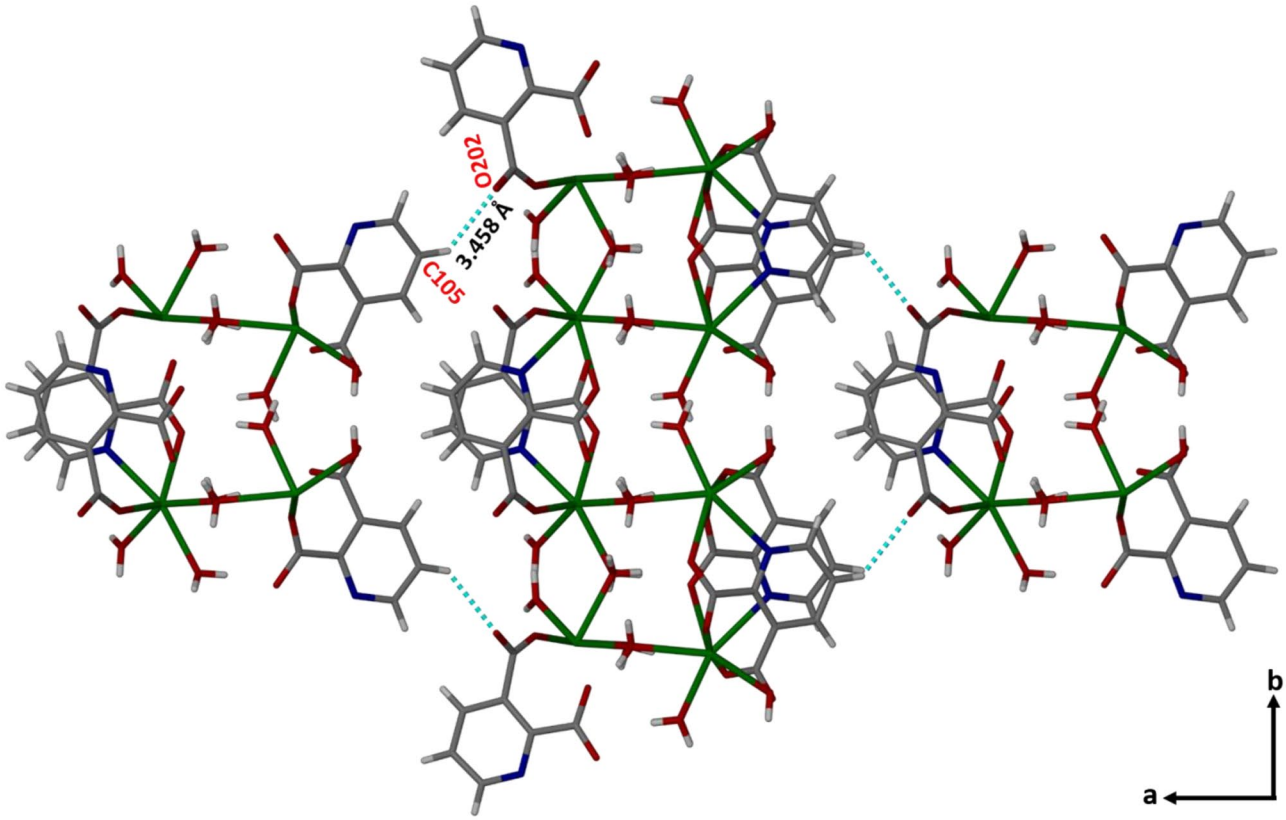


Fig. 6 Crystal packing of **2** showing C−H···O hydrogen bonding interactions when viewed along *c*-axis

CaO residue was left until 800 °C. The melting points were found to range between 248–250 °C and 186–188 °C for 2,6-H_2pdc and 2,3-H_2pdc ligands respectively. The results of the thermal analysis show that the compounds are more thermally stable than some metal coordination compounds of pyridinedicarboxylate [9, 12]. However, the thermal stability of beyond 400 °C was reported for some calcium coordination compounds [19, 35].

DFT studies

Optimized molecular structure

The calculated bond parameters are presented in Table S2. **1** presents an underestimation of Ca-O (H_2O) bond lengths (~ 2.424 Å) compared to **2** (~ 2.543 Å), and this is due to the varying electron donation groups influenced by intramolecular interaction (H-bonding) within **2**.

HOMO–LUMO energy gap

The HOMO − LUMO gap describes the stability of molecules, and it predicts reactivity between species by providing the electrical transport properties as well as electron carrier and mobility in molecules [36–38]. The calculated HOMO and LUMO energies of **1** and **2** are summarized in Table 2. As shown in Fig. 9, the charge density distribution of **1** illustrates that the HOMO density is mainly located around the 2,6-pyridinedicarboxylic acid (2,6-H_2pdc) ligand, especially their nitrogen atom/imine and caboxylic groups, there are some indications that calcium atom may partly contribute to HOMO (Fig. 9). The LUMO density is localized around the 2,6-pyridinedicarboxylic acid (2,6-H_2pdc) ligand. With **2**, the HOMO density is mainly located around the 2,3-pyridinedicarboxylic acid (2,3-H_2pdc) ligand and the LUMO density is centred on the 2,3-pyridinedicarboxylic acid (2,3-H_2pdc) ligand (around nitrogen and oxygen atoms) and the calcium atom (Fig. 10). Compound **2** displayed the smallest energy gap (5.156 eV) which is indicative of the softest molecule with better polarizability. Similarly, the lowest LUMO energy (E_{LUMO} = 1.874 eV), which means that it can be the best acceptor of electrons [39]. **1** is characterized with an energy gap (ΔE_{gap} = 9.221 eV), and this may indicate a molecule with high excitation energy, good stability and a high chemical hardness (Table 2). The HOMO − LUMO orbitals in **1** and **2** are presented in Figs. 10 and 11, respectively.

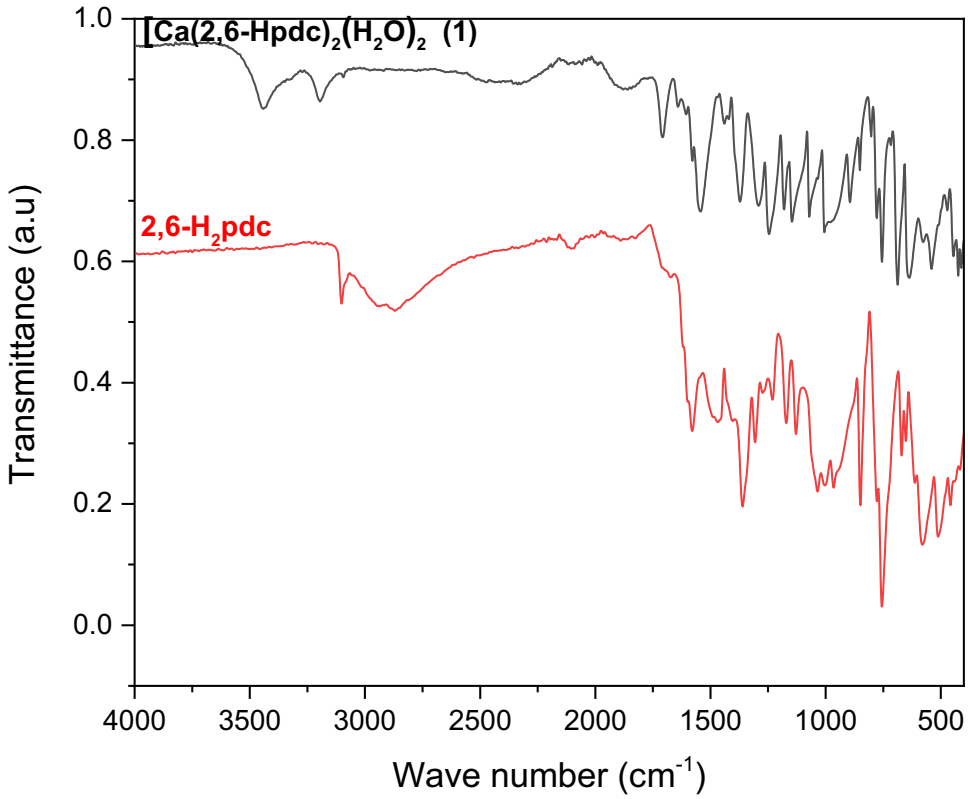


Fig. 7 FTIR spectra of (**1**) and its ligand

The ionization potential (I), electron affinity (A), chemical potential (μ), electronegativity (χ), global hardness (η), global softness (S) and global electrophilicity (ω) values were calculated using the HOMO and LUMO energy values [40]. The HOMO energy (E_{HOMO}) is related to ionization potential (I) by Koop-man's theorem and LUMO energy (E_{LUMO}) is related to electron affinity (A) [41] by the following relations:

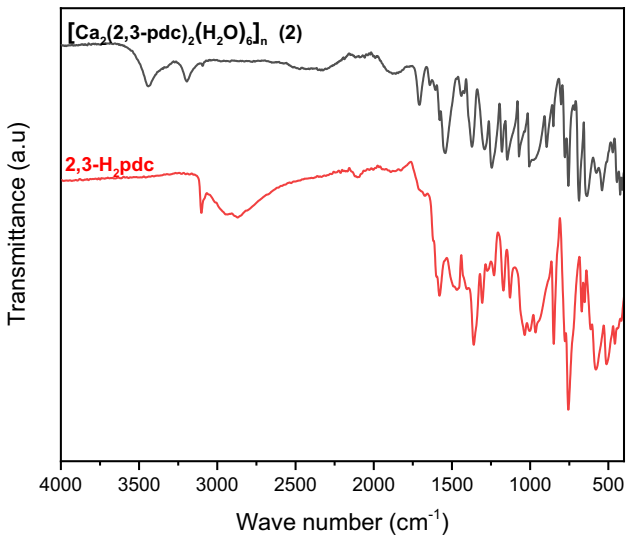


Fig. 8 FTIR spectra of (**2**) and its ligand

$$\text{Ionization potential } (I) = -E_{HOMO} \tag{1}$$

$$\text{Electron affinity } (A) = -E_{LUMO} \tag{2}$$

Absolute electronegativity (χ) is related to average value of HOMO and LUMO energies defined by Mulliken [42].

$$\text{Electronegativity } x = \frac{I + A}{2} \tag{3}$$

The softness (S) is reciprocal of the hardness (η) [43]

$$\text{Global hardness, } \eta = \frac{I - A}{2} \tag{4}$$

$$\text{Global softness, } S = \frac{1}{\eta} \tag{5}$$

Parr et al. defined global electrophilicity index (ω) [44]

$$\text{Electrophilicity index } \omega = \frac{\mu^2}{2\eta} \tag{6}$$

where μ is the chemical potential takes the average value of ionization potential (I) and electron affinity (A) [45].

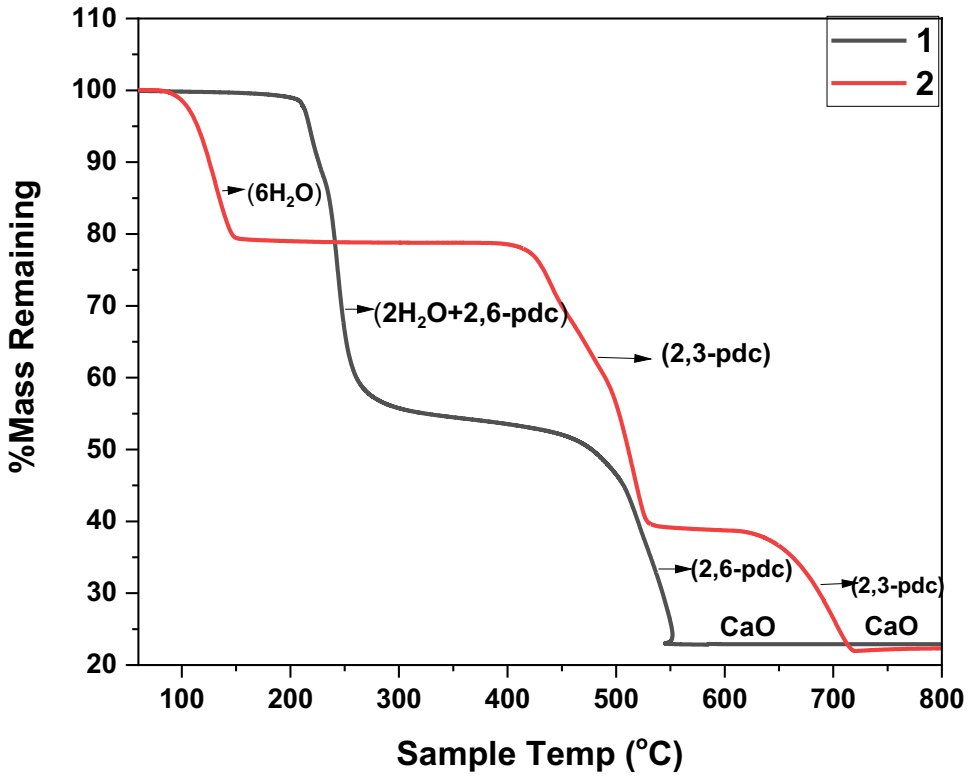


Fig. 9 TGA curves of **1** and **2**

Table 2 Quantum chemical descriptors of **1** and **2**

Parameter	1	2
E_{HOMO} (eV)	−7.213	−3.282
E_{LUMO} (eV)	2.008	1.874
ΔE_{gap} (eV)	9.221	5.156
I (eV)	7.213	3.282
A (eV)	−2.008	−1.874
μ (eV)	−2.603	−0.704
χ (eV)	2.603	0.704
η (eV)	4.611	2.578
S (eV)	0.217	0.388
ω (eV)	0.734	0.096

$$\text{Chemical potential } \mu = -\left(\frac{I+A}{2}\right) \tag{7}$$

The lowest value of the potential ionization ($I = 3.282$ eV) for **2** confirms that it is the better electron donor [46]. Chemical hardness and softness value of **1** ($\eta = 4.611$ eV, $S = 0.217$ eV) is greater (lesser) than that of **2**, respectively. Thus, it shows a molecule which is less reactive in nature. **1** possesses higher electronegativity value ($\chi = 2.603$ eV) than **2**, hence making it a better electron acceptor. The value of ω for **1** ($\omega = 0.734$ eV) indicates that it is the stronger electrophile.

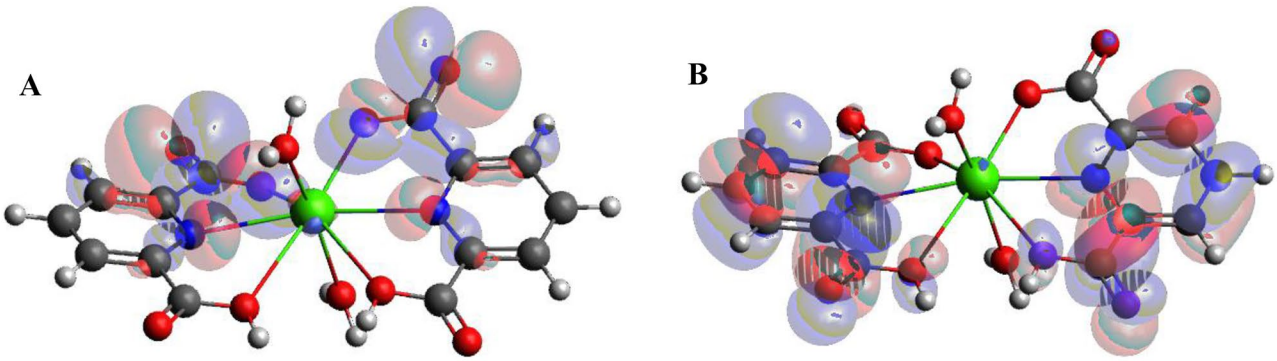


Fig. 10 Frontier molecular orbitals (**A** HOMO and **B** LUMO) for the optimized structure of **1** (green, blue, yellow and grey colours represent calcium, nitrogen, and carbon atoms respectively)

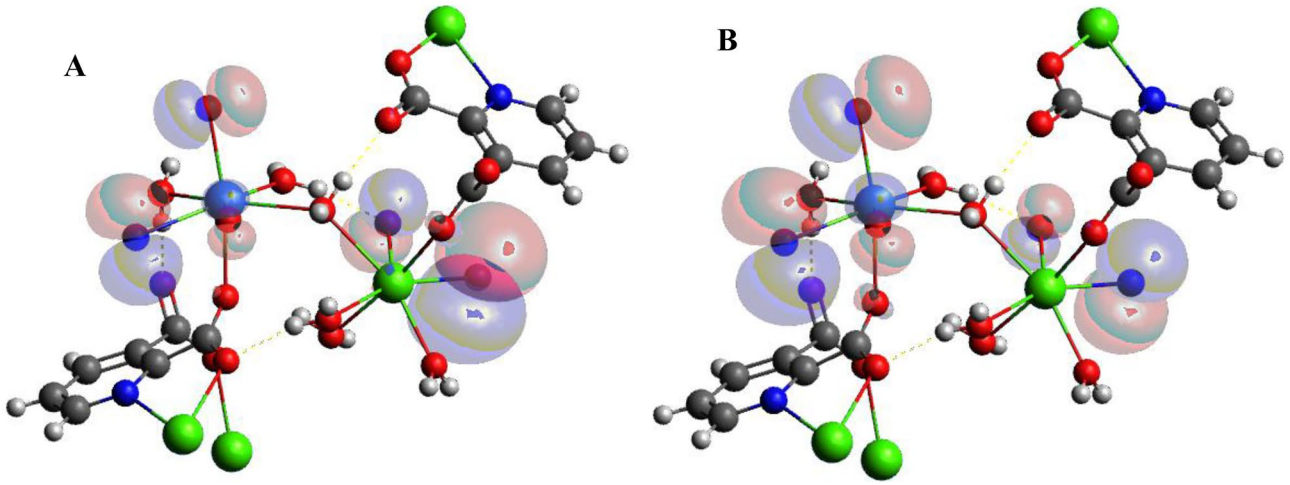


Fig. 11 Frontier molecular orbitals (**A** HOMO and **B** LUMO) for the optimized structure of **2**. (green, blue, yellow and grey colours represent calcium, nitrogen, and carbon atoms respectively)

Conclusions

Two calcium coordination compounds of dipicolinate and quinolinate ligands were successfully synthesized. Structural characterization revealed that the Ca(II) ion in **1** interacts with adjacent carboxylate groups via strong intermolecular hydrogen bonds. On the other hand, **2** revealed two calcium centres, Ca1 and Ca2. For the two compounds, the torsional angles between the carboxylate group and the aromatic ring showed that they exhibit antiperiplanar conformation. Optimized molecular structures by DFT simulations are comparable to the crystal structure geometry obtained by X-ray diffraction. Furthermore, theoretical calculations of the HOMO–LUMO energies confirmed that compound **1** is a better electron acceptor with less reactivity while compound **2** with smaller energy gap is more reactive.

Supplementary information The online version contains supplementary material available at https://doi.org/10.1007/s11224-022-01935-x.

Acknowledgements The School of Chemistry, University of Nottingham and the University of Warwick's Research Technology Platforms, for the provision of facilities for the analysis of the compounds. We are grateful to the Center for High Performance Computing (CHPC), Capetown, South Africa for providing the platform to carry out molecular modelling studies using the Gaussian09 software.

Author contribution Adedibu Clement Tella: conceptualization, supervision, writing–review, editing and design of study. Adetola Christianah Oladipo: data curation, formal analysis, methodology, writing–original draft. Victoria Tosin Olayemi: data curation, formal analysis, methodology, writing–original draft. Allen Gordon: DFT modelling, writing–review, editing and design of study. Adeniyi Sunday Ogunlaja: DFT modelling, Supervision, writing–review, editing and design of study. Lukman Olawale Alimi: conceptualization, supervision, writing–review, editing and design of study. Stephen Argent: single crystal analyses and interpretation, supervision, writing–review and editing. Robert Mokaya: conceptualization, supervision, writing–review, editing and design of study. Guy Clarkson: single crystal analyses and interpretation, supervision, writing–review and editing. Richard Walton: conceptualization, supervision, writing–review, editing and design of study.

Funding The authors appreciate the Royal Society of Chemistry for funding.

Data availability CCDC 1,999,478 and CCDC 1,954,758 contains the crystallographic data of $Ca(H(2,6\text{-pyr}))_2(H_2O)_2$ **1** and $[Ca_2(2,3\text{-pyr})_2(H_2O)_6]_n$ **2** respectively. These data can be obtained free of charge from the Cambridge Crystallographic Data Centre via https://www.ccdc.cam.ac.uk/structures.

Code availability The datasets and codes for DFT modeling generated during the current study will be made available upon request.

Declarations

Conflict of interest There are no conflicts to declare.

References

1. Li D, Xu HQ, Jiao L, Jiang HL (2019) Metal-organic frameworks for catalysis: state of the art, challenges, and opportunities. EnergyChem 1:100005. https://doi.org/10.1016/j.enchem.2019.100005
2. Li B, Wen HM, Yu Y, Cui Y, Zhou W, Chen B, Qian G (2018) Nanospace within metal–organic frameworks for gas storage and separation. Mater Today Nano 2:21–49. https://doi.org/10.1016/j.mtnano.2018.09.003
3. Han L, Qin L, Xu L, Zhou Y, Sun J, Zou X (2013) A novel photochromic calcium-based metal–organic framework derived from a naphthalene diimide chromophore. Chem Commun 49:406–408
4. Noro SI, Mizutani J, Hijikata Y, Matsuda R, Sato H, Kitagawa S, Sugimoto K, Inubushi Y, Kubo K, Nakamura T (2015) Porous coordination polymers with ubiquitous and biocompatible metals and a neutral bridging ligand. Nat Commun 6:1–9. https://doi.org/10.1038/ncomms6851

5. Fromm KM (2008) Coordination polymer networks with s-block metal ions. Coord Chem Rev 252:856–885. https://doi.org/10.1016/j.ccr.2007.10.032
6. Bar-Shir A, Gilad AA, Chan KW, Liu G, van Zijl PC, Bulte JW, McMahon MT (2013) Metal ion sensing using ion chemical exchange saturation transfer 19F magnetic resonance imaging. J Am Chem Soc 135:12164
7. Begouin JM, Niggemann M (2013) Niggemann. Chem Eng J 19:8030
8. Yeh CT, Lin WC, Lo SH, Kao CC, Lin CH, Yang CC (2012) Cryst Eng Comm 14:1219
9. Lazarescu A, Shova S, Bartolome J, Alonso P, Arauzo A, Balu AM, Simonov YA, Gdaniec M, Turta C, Filoti G, Luque R (2011) Heteronuclear (Co-Ca, Co-Ba) 2,3-pyridinedicarboxylate complexes: synthesis, structure and physico-chemical properties. Dalt Trans 40:463–471. https://doi.org/10.1039/c0dt00858c
10. An CX, Lu YC, Shang ZF, Zhang ZH (2008) Syntheses and crystal structures of the metal complexes based on pyrazolecarboxylic acid ligands. Inorg Chim Acta 361:2721
11. Ghosh A, Rao KP, Sanguramath RA, Rao CNR (2009) Two-and three-dimensional lead-1H-imidazole-4, 5-dicarboxylates. J Mol Struct 927:37
12. Abdolmaleki S, Ghadermazi M, Ashengroph M, Saffari A, Sabzkohi SM (2018) Cobalt (II), zirconium(IV), calcium(II) complexes with dipicolinic acid and imidazole derivatives: X-ray studies, thermal analyses, evaluation as in vitro antibacterial and cytotoxic agents. Inorganica Chim Acta 480:70–82. https://doi.org/10.1016/j.ica.2018.04.047
13. Wang N, Yue S, Wu H, Li Z, Li X, Liu Y (2010) Hydrothermal synthesis, crystal structure and magnetic characterization of two 4f–3d heterometallic coordination polymers. Inorganica Chim Acta 363:1008–1012. https://doi.org/10.1016/j.ica.2009.12.022
14. Kitagawa S, Kitaura R, Noro SI (2004) Functional porous coordination polymers. Angew Chemie - Int Ed 43:2334–2375. https://doi.org/10.1002/anie.200300610
15. Yuoh ACB, Agwara MO, Yufanyi DM, Conde MA, Jagan R, Oben Eyong K (2015) Synthesis, crystal structure, and antimicrobial properties of a novel 1-D cobalt coordination polymer with dicyanamide and 2-aminopyridine. Int J Inorg Chem 2015:1–8. https://doi.org/10.1155/2015/106838
16. Volkringer C, Loiseau T, Férey G, Warren JE, Wragg DS, Morris RE (2007) A new calcium trimellitate coordination polymer with a chain-like structure. Solid State Sci 9:455–458. https://doi.org/10.1016/j.solidstatesciences.2007.04.002
17. Sun Y, Sun Y, Zheng H, Wang H, Han Y, Yang Y, Wang L (2016) Four calcium(II) coordination polymers based on 2,5-dibromoterephthalic acid and different N-donor organic species: syntheses, structures, topologies, and luminescence properties. CrystEngComm 18:8664–8671. https://doi.org/10.1039/c6ce01709f
18. Xu X, Yan S, Hu F, Zhao W, Shuai Q (2016) Calcium coordination compounds based on phenoxyacetic acids: microwave synthesis, thermostability and influences on the crystal structures of chlorine substituent group on ligands. J Coord Chem 69:541–550. https://doi.org/10.1080/00958972.2015.1126259
19. Raja DS, Luo JH, Chang TG, Lo SH, Wu CY, Lin CH (2013) Synthesis, crystal structure, and luminescence properties of a new calcium(II) coordination polymer based on L-malic acid. J Chem 41:980243. https://doi.org/10.1155/2013/980243
20. Srinivasan BR, Shetgaonkar SY, Ghosh NN (2011) Synthesis and characterization of calcium(II) coordination polymers based on phenylacetic acid. J Coord Chem 64:1113–1124. https://doi.org/10.1080/00958972.2011.562289
21. Appelhans LN, Kosa M, Radha AV, Simoncic P, Navrotsky A, Parrinello M, Cheetham AK (2009) Phase selection and energetics in chiral alkaline earth tartrates and their racemic and meso analogues: synthetic, structural, computational and calorimetric studies. J Am Chem Soc 131:15375
22. Dietzel PC, Blom R, Fjellvag H (2009) Coordination polymers based on the 2,5-dihydroxyterephthalate ion and alkaline Earth metal (Ca, Sr) and manganese cations. Z Anorg Allg ChemAnorg Allg Chem 635:1953
23. Tran DT, Chu D, Oliver AJ, Oliver SRJ (2009) Synthesis and characterization of strontium 1,3,5-benzenetricarboxylate, [Sr3(1,3,5-BTC)2(H2O)4]·H2O. Inorg Chem Commum 12:351
24. Dolomanov OV, Bourhis LJ, Gildea RJ, Howard JAK, Puschmann H (2009) OLEX2: a complete structure solution, refinement and analysis program. J Appl Crystallogr 42:339–341. https://doi.org/10.1107/S0021889808042726
25. MacRae CF, Sovago I, Cottrell SJ, Galek PTA, McCabe P, Pidcock E, Platings M, Shields GP, Stevens JS, Towler M, Wood PA (2020) Mercury 4.0: from visualization to analysis, design and prediction. J Appl Crystallogr 53:226–235. https://doi.org/10.1107/S1600576719014092
26. Sheldrick GM (2015) SHELXT - integrated space-group and crystal-structure determination. Acta Crystallogr Sect A Struct Chem A71:3–8
27. Sheldrick GM (2015) Crystal structure refinement with SHELXL. Acta Crystallogr Sect C Struct Chem 71:3–8. https://doi.org/10.1107/S2053229614024218
28. Frisch MJ, Trucks GW, Schlegel HB, Scuseria GE, Robb MA, Cheeseman JR, Scalmani G, Barone V, Mennucci B, Petersson GA et al (2016) GAUSSIAN 16
29. Becke AD (1993) Density-functional thermochemistry. III. The role of exact exchange. J Chem Phys 98:5648–5652. https://doi.org/10.1063/1.464913
30. Téllez VC, Gaytán BS, Bernès S, Vergara EG (2002) The supramolecular structure of pyridine-2,6-dicarboxylic acid. Acta Crystallogr Sect C Cryst Struct Commun 58:o228–o230. https://doi.org/10.1107/S0108270102002172
31. Tripuramallu BK, Manna P, Reddy SN, Das SK (2012) Factors affecting the conformational modulation of flexible ligands in the self-assembly process of coordination polymers: synthesis, structural characterization, magnetic properties, and theoretical studies. Cryst Growth Des 12:777–792 . https://doi.org/10.1021/cg201111r
32. Li QY, Yang GW, Shen L, He MH, Shen W, Gu K, Jin JN (2012) Magnesium(II), calcium(II), and barium(II) coordination compounds constructed by 1h-tetrazolate-5-acetic acid ligand. Zeitschrift fur Anorg und Allg Chemie 638:826–831. https://doi.org/10.1002/zaac.201100514
33. Scaldini FM, Correa CC, Yoshida MI, Krambrock K, Machado FC (2014) 2-D coordination polymers of copper and cobalt with 3,4-pyridinedicarboxylic acid: Synthesis, characterization, and crystal structures. J Coord Chem 67:2967–2982. https://doi.org/10.1080/00958972.2014.959002
34. Tobias RS (1979) Infrared and Raman spectra of inorganic and coordination compounds (Nakamoto, Kazuo), fifth. Wiley-Interscience, New York
35. Al-Terkawi AA, Scholz G, Prinz C, Zimathies A, Emmerling F, Kemnitz E (2018) Hydrated and dehydrated Ca-coordination polymers based on benzene-dicarboxylates: mechanochemical synthesis, structure refinement, and spectroscopic characterization. CrystEngComm 20:946–961. https://doi.org/10.1039/c7ce01906h
36. Ogunlaja AS, Hosten E, Tshentu ZR (2014) Dispersion of asphaltenes in petroleum with ionic liquids: evaluation of molecular interactions in the binary mixture. Ind Eng Chem Res 53:18390–18401. https://doi.org/10.1021/ie502672q
37. Olalekan TE, Ogunlaja AS, VanBrecht B, Watkins GM (2016) Spectroscopic, structural and theoretical studies of copper(II) complexes of tridentate NOS Schiff bases. J Mol Struct 1122:72–79. https://doi.org/10.1016/j.molstruc.2016.05.098

38. Rathi PC, Ludlow RF, Verdonk ML (2019) Practical high-quality electrostatic potential surfaces for drug discovery using a graph-convolutional deep neural network. J Med Chem. https://doi.org/10.1021/acs.jmedchem.9b01129
39. Tella AC, Olayemi VT, Adekola FA, Oladipo AC, Adimula VO, Ogar JO, Hosten EC, Ogunlaja AS, Argent SP, Mokaya R (2021) Synthesis, characterization and density functional theory of copper(II) complex and cobalt(II) coordination polymer for detection of nitroaromatic explosives. Inorganica Chim Acta 515:120048. https://doi.org/10.1016/j.ica.2020.120048
40. Saravanan S, Balachandran V (2014) Quantum chemical studies, natural bond orbital analysis and thermodynamic function of 2,5-dichlorophenylisocyanate. Spectrochim Acta - Part A Mol Biomol Spectrosc 120:351–364. https://doi.org/10.1016/j.saa.2013.10.042
41. Politzer P, Abu-Awwad F (1998) A comparative analysis of Hartree-Fock and Kohn-Sham orbital energies. Theor Chem Acc 99:83–87. https://doi.org/10.1007/s002140050307
42. Mulliken RS (1934) A new electroaffinity scale; together with data on valence states and on valence ionization potentials and electron affinities. J Chem Phys 2:782–793. https://doi.org/10.1063/1.1749394
43. Hoffmann R (1988) Solids and surfaces: a chemist's view of bonding in extended structures. VCH Publishers, New York
44. Parr RG, Szentpály LV, Liu S (1999) Electrophilicity index. J Am Chem Soc 121:1922–1924. https://doi.org/10.1021/ja983494x
45. Padmanabhan J, Parthasarathi R, Subramanian V, Chattaraj PK (2007) Electrophilicity-based charge transfer descriptor. J Phys Chem A 111:1358–1361. https://doi.org/10.1021/jp0649549
46. Abbaz T, Bendjeddou A, Villemin D (2018) Structural studies, NBO analysis and reactivity descriptors of π-Extended tetrathiafulvalene (exTTF) connected to thiophene derivative. Arch Curr Res Int 14:1–13. https://doi.org/10.9734/acri/2018/41529

Publisher's note Springer Nature remains neutral with regard to jurisdictional claims in published maps and institutional affiliations.